https://doi.org/10.46813/2023-148-161

ACOUSTIC DIAGNOSTICS OF COOLANT PHASE TRANSITIONS IN A SUPERCRITICAL CONVECTION WATER LOOP

O.S. Bakai, V.M. Boriskin, V.V. Churikov
National Science Center "Kharkov Institute of Physics and Technology", Kharkiv, Ukraine
E-mail: churikov.v@kipt.kharkov.ua

When choosing a coolant for 4th generation reactors, water in a supercritical state is studied. The acoustic method was chosen as one of the research methods, it is optimal under the conditions. Requirements for the device, implementation, and work results are described.

PACS: 85.40.-e; 89.20.Bb

INTRODUCTION

One of the promising types of nuclear reactors of the next generation are supercritical water-cooled reactors (Super-Critical Water-cooled Reactor, SCWR), which must operate under conditions of supercritical coolant pressure and high temperature. The water coolant is in a state above the critical point (Tpc, Ppc) = (374°C, 22.1 MPa) water. SCWR has a number of advantages such as simpler construction and higher thermal efficiency. The development of SCWR is carried out in different countries in accordance with the international program "Generation IV" [1 - 6]. Design characteristics of prospective SCWRs being developed from review papers [7, 8], are given in Table. Single-loop reactors are mainly designed.

One of the tools for simulating and studying the processes occurring in SCWR channels are loops with convection or forced circulation of the coolant [9 - 11]. In such loops, the studied samples of materials for reactors are exposed to supercritical water and radiation exposure [12].

Below we discuss the possibility of controlling the processes occurring in the Super-Critical Water Loop (SCWL), with radiation exposure using acoustic methods [13].

1. SCWL AT THE NATIONAL SCIENCE CENTER "KHARKOV INSTITUTE OF PHYSICS AND TECHNOLOGY" (NSC KIPT)

Electron Irradiation Test Facility (EITF) NSC KIPT is constructed to conduct experiments on the corrosion of structural materials in molten salts [14] and in aqueous environments [15] under irradiation. Currently experiments are focused on assessment of corrosion resistance of advanced structural materials of nuclear reactors in circulation loop with water in sub- and super-critical states under electron and γ-irradiation. The developed methodology provides research of Irradiation Assisted Corrosion (IAC) and the Irradiation Assisted Stress Corrosion Cracking (IASCC). Development of a research methodology of the Irradiation Assisted Fatigue Corrosion (IAFC) is in progress. The Electron Irradiation Test Facility contributed to this program over the past two decades. The core of the Facility is the LEA-10 electron linac (10 MeV/10 kWe). For the SCWR related tasks, the EITF natural convection principle based SCWL (Figs. 1, 2) was put into operation in 2012 [16, 17].

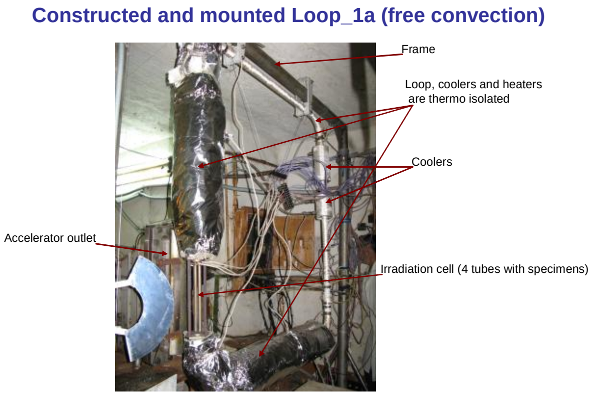

Fig. 1. Photo of Loop-1a inside LEA-10 chamber

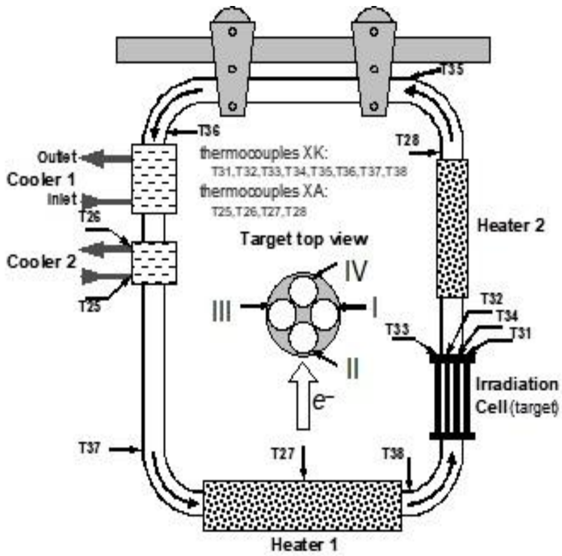

Fig. 2. Water circulation loop diagram

Further EITF SCWL specifically focused on investigations of the mechanical stress impact on materials corrosion under irradiation. An appropriate upgrade of the SCW IC "LOOP-1b" design (see ref. [18]) has resulted in the completion (2019) of the next irradiation experiment specifically devoted to the evaluation of IAC and IASCC of SS 12X18H10T coupons in SCW under controlled static mechanical load. And in 2021, in the specially created SCWL "LOOP-1c" [19], samples of SS 12X18H10T were irradiated in SCW under controlled dynamic mechanical load.

Technical characteristics of prospective SCWR projects

Characteristic	SCWR-R, Korea	SCLWR, Japan	SCWRINEEL, USA	U1tra CANDU+, Canadian SCWR, Canada	HPLWR, Europe	CSR-1000, China	SCFR, Japan
Thermal capacity, MW	3.989 (3.846)	2.273 (2.740)	3.570 (3.575)	2.540	2188 (2 300)	2.284	3.832 (3.893)
Electric power, MW	1739 (1700)	950 (1217)	1.600	1220 (1140)	1000	1.000	1698 (1.728)
Efficiency, %	43.7 (44)	42 (44.4)	44.8	48 (45)	43.5	43	44.3 (44.4)
Feed water temperature, °C	350 (280)	280	280	350	280	280	280
Hot steam temperature, °C	510 (508)	508	500	625	508 (500)	500	523 (526)
Hot steam pressure, MPa	25	25	25	25	25	25	25
Spectrum of neutrons	T	T	T	T	T	T	F
Feed water consumption, kg/s	2518 (1862)	1816 (1342)	1843	1312 (1320)	1113 (1160)	1 177	1897 (1694)

Note. T is the thermal spectrum of neutrons; F – fast neutron spectrum; data [7] in brackets; the period of operation is provided from 60 to 75 years (Canadian SCWR).

In 2012-2021, with the help of the SWCL created at the NSC KIPT, three sessions of corrosion studies of reactor materials under irradiation were carried out. The duration of the sessions is 500…600 h. Samples of the studied materials were placed in four-channel irradiation chambers (IC) in special cassettes (Figs. 3-5).

Thermal processes occurring in IC LOOP-1 are studied in [17, 18]. The prescribed and the facility control system and operators sustained characteristic temperature of the coolant circulation, Tin = 360°C was deliberately set smaller critical Tc = 374°C temperatures of water. It was measured by an array of thermocouples placed outside the irradiation zone (direct thermometry is problematical inside it). The System Thermal Hydraulic (STH) calculations reveal the cross-section averaged temperature growth to 368°C before the IC outlet, and the subsequent cooling. The readings of the post-outlet thermocouples at the IC outer surface were 364°C for the IC channels II and III (see Fig. 2) and 350°C for tubes I and IV. By and large, this agrees well with the STH prediction which also well describes possible gradual cooling of a flow by the end of weakly irradiated channels (Fig. 9 of ref. [17]). Generally, coolant circulated in a narrow lower vicinity of supercritical transition. However, under e-irradiation, the remote optical pyrometry measurements [19] revealed temperatures of 400…420°C >> Tpc at the aircooled external surface of the IC.

In ref. [17], it was shown that massive IC internals also can be about 10…15 K hotter than the STH predicted reference temperature of a coolant. Thus, the supercritical transition occurs directly inside the IC near the irradiated samples.

During long sessions of irradiation, technological shutdowns of LEA systems are possible, for various reasons [20]. When the electron beam is switched off, the IC cools down. The water pressure in the loop decreases sharply (Fig. 6). Phase transitions of water to the supercritical state in the channels of the IC stop.

Fig. 3. Irradiation Cell

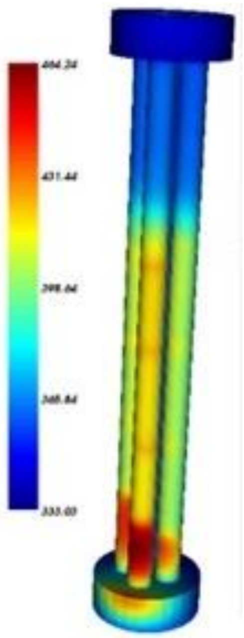

Fig. 4. Temperature distribution in the Irradiation Cell

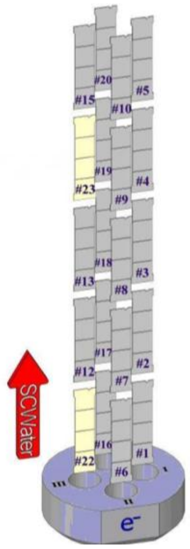

Fig. 5. Placement of samples in cassettes of IC

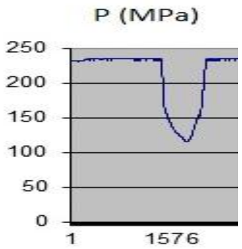

Fig. 6. Graph of pressure change in the loop 17-08-21. The duration of the event (pressure drop below 200 atm) is about 31 min 40 s. The event starts around 21-28-00 and ends at 21-59-40

When the beam is turned on, the IC heats up, the pressure in the loop rises above the critical point. Accordingly, the phase transitions of water to the supercritical state in the channels of the IC are renewed.

In the irradiation session of 2021, the convection loop was equipped with an acoustic channel [21]. The results of studies of acoustic effects occurring in the convection loop "Loop-1c" during phase transitions of the coolant are discussed below.

2. EXPERIMENTAL TECHNIQUE

2.1. HARDWARE INTERACTION

Ethernet network was chosen as the main method of communication between devices, as it allows data transmission at distances greater than 100 m and has sufficient bandwidth to transmit the required amount of data.

The decision was made to choose STM32F4-Discovery as the basis for the device, since the microcontroller on this board has a sufficient amount of memory, a fairly high frequency of operation (168 MHz), supports the RMII interface, which allows the use of Ethernet network adapters (Fig. 10), and is distinguished by high-precision 12-bit ADC, which allows you to distinguish the signal level with an accuracy of up to 8 mV. The next step was the selection of the microphone module: the MAX9814 has proven itself as a quality microphone module, distinguished by ease of connection and sound registering quality. To work with an Ethernet network was the DP83848 module is selected. The power source is a mobile phone charger that supplies 5 V and 1 A current output.

As a server, a computer needed with the following minimum possible characteristics:

- OS: Windows 7 Professional x64 or Windows 10 Professional x64;
- CPU: dual-core, 2.8 GHz, or better;
- RAM: DDR3 8 GB or better;
- free space: 10 MB or more.

The following is chosen as the most appropriate scheme of interaction:

1. The microphone (Fig. 7) is connected to the supercritical water convection loop using a metal rod in order to avoid overheating and ensure better transmission of the acoustic signal.

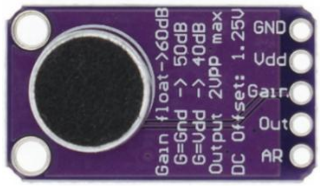

Fig. 7. MAX9814 module

This module is responsible for converting acoustic waves into electromagnetic waves and has the following characteristics:

- supply voltage: 2.7…5.5 V at a current of 30 mA;
- output: 2 Vpp at 1.25 V offset;
- frequency response: 20 Hz…20 kHz;
- programmable attack and decay ratio;
- temperature range -40...+85°C.

2. The microphone is connected using a twisted pair to the STM32F4-Discovery (Fig. 8) microcontroller module. This module is responsible for receiving an analog signal, converting it to a digital one, accumulating data and transferring it to the server application via the Ethernet network. The maximum clock frequency is 168 MHz, the polling frequency of the ADC is 32768 Hz. The supply voltage is 5 V with a current of 300 mA.

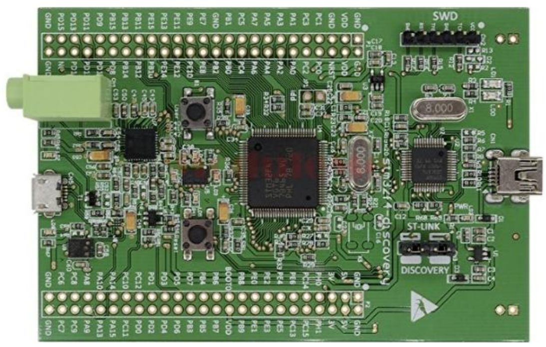

Fig. 8. STM32F4-Discovery module

3. The microcontroller module transmits the recorded data in the form of a TCP packet to the Ethernet adapter board DP83848 (see Fig. 9) for further data transfer to the server via the Ethernet network.

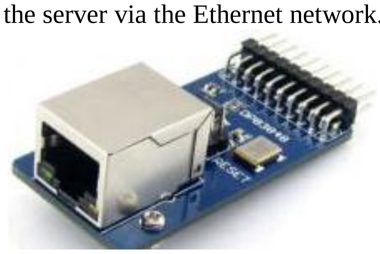

Fig. 9. DP83848 module

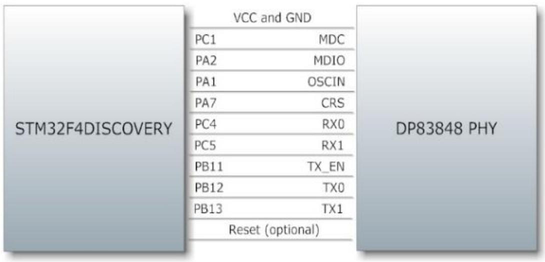

Fig. 10. Device interaction scheme

This module is designed for communication of a microcontroller module with an Ethernet network, has the following characteristics:

- network support: 10/100 Mbit;
- standard: 802.3u MII/RMII;
- supply voltage: 3.3 V;
- consumed power: <270 mW.

4. The server accepting incoming connections, receives information packets and distributes the accumulated information to all clients, closes the connections.

5. The client who received the information saves the received information in CSV format files at certain intervals. Also, the client performs transformation on the data using the FFT algorithm and displays the received signal spectrum or raw data on the screen.

In this way, the fulfillment of all conditions and tasks is ensured. Users can receive acoustic data at a considerable distance, analyze the operation of the magnetic drive unit using acoustic signal spectrum data.

2.2. DEVICE MODULE CONNECTION DIAGRAM

This device is based on 3 modules: STM32F4-Discovery, DP83848 and MAX9814. The STM32F4-Discovery motherboard is connected to the DP83848 adapter using the RMII interface (Fig. 11):

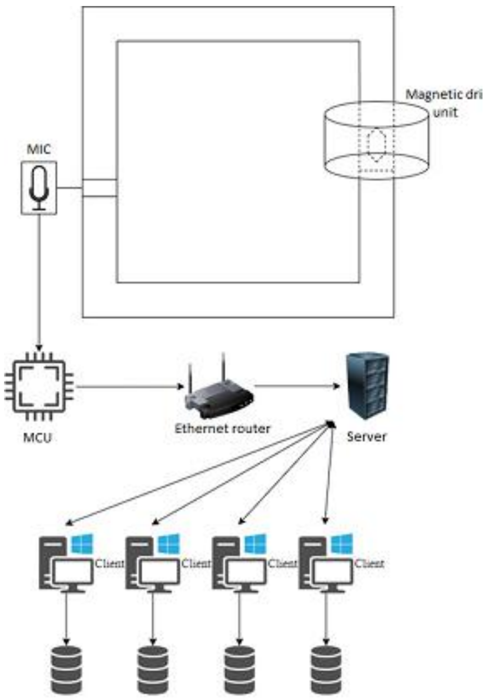

Fig. 11. Connection diagram of STM32F4-Discovery and DP83848

The MAX9814 microphone module receives power from the STM32F4-Discovery board and transmits an analog signal to the microcontroller's ADC (Fig. 12):

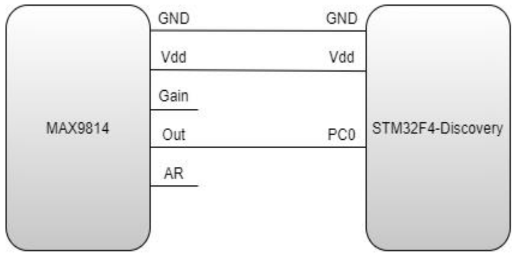

Fig. 12. STM32F4-Discovery and MAX9814 connection diagram

The device has been tested and calibrated before installation. The frequencies of the sound generated corresponded to the frequencies detected by the device.

2.3. DESCRIPTION OF THE SOFTWARE COMPLEX

A client-server architecture was chosen to fulfill the tasks. Based on the existing material and technical base, applications compatible with the Windows 7/10 OS were developed.

Spectrum! TCP Server:

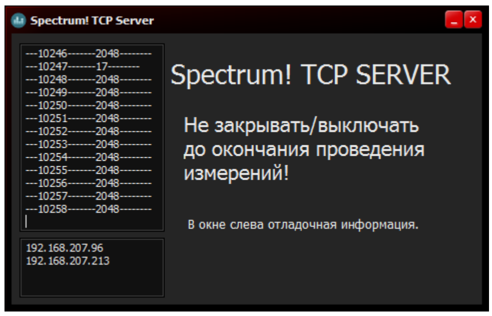

Fig. 13. Spectrum! TCP Server interface

The TCP server (Fig. 13) takes up 3.7 MB of disk space and is designed to receive data from the microcontroller module and distribute it to clients. The data update period is 1 second. In case of quite active data exchange with clients, the server needs a fairly wide data channel calculated on average of 600 kB/s for each client. The maximum number of connections is set to 500. Application also displays request flow and IP addresses of connected clients. For better use it can be hidden to the tray, so the new connected clients will be shown as a balloon-popup.

Spectrum!

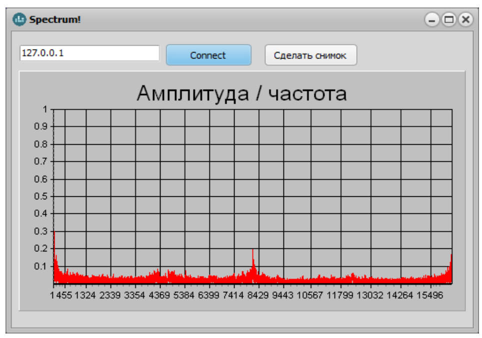

Fig. 14. Spectrum! Interface

Client application (Fig. 14) designed for recording data, visualization of current data. Data is saved in CSV format for easier processing and compatibility with other applications.

The graphic sizes adapt to any monitor sizes and resolutions. Also, the graphic is easily scaled in any area convenient for the user, there is an option to choose a recording period and an instant recording button for urgent recording in emergency situations.

Every second, the application receives 32768 records in the range from 0 to 4096, which corresponds to the amplitude received by the microphone. Next, using the FFT algorithm, we get a spectrum that allows us to estimate the spectral pattern of the existing signal from 15 to 16384 Hz (according to the minimum sensitivity threshold of the microphone and the Nyquist frequency). The user can also switch between spectrum and raw data observation modes.

Spectrum! ReMember

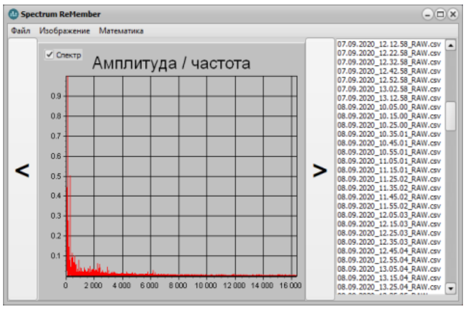

Fig. 15. Spectrum! ReMember interface

The application (Fig. 15) is intended for visualization, conversion and processing of already saved data.

For the application to work, you need to place it in the folder with saved data and run it. This application provides an opportunity to save graphics in full or scaled parts in BMP format. The application can currently be used to compare, find the difference between 2 graphs. Display data both in raw form and in the form of a spectrum using the FFT algorithm.

All the above parts of the complex are fully compatible with operating systems Windows 7/10 Professional x32/x64.

Software for STM32F4-Discovery:

The STM32F4-Discovery board is equipped with a 12-bit ADC and an RMII interface that allows you to operate the MAX9814 microphone module and the DP83848 Ethernet adapter.

When receiving power, the STM32F4-Discovery board initiates the Ethernet adapter and tries to connect to the server, if the server is unavailable, the indicator turns on – the red LED blinks, if the server is unavailable for too long – the board reboots, which allows to reset all connections and start the initialization from the beginning. If the communication line is not available – the cable is damaged or the cable is missing – the board turns on the red LED and waits for a correct connection. If the connection with the server has taken place and the data is transferred successfully, the board turns on the indication – the green LED flashes.

The time required to continue data transfer after the device is turned off and the power is restored is 2…3 s. In case of critical errors due to network malfunction or incorrect requests from the server or overload in cases of network flooding, the device reboots, resetting connections, makes attempts to reconnect to the server and, if successful, continues to transfer data. Accumulation of the data received by the ADC takes place using two buffers: at first the first one is filled, then it is queued for transmission and transmitted, while the second one is filled. Such a carousel of buffers allows you to transfer data without any data loss.

The device also supports hot-swap of the microphone module, which can fail due to excess moisture, radiation, or power surges.

3. RESULTS RECEIVED FROM HARDWARE AND SOFTWARE COMPLEX

While the device was in operation, sound was recorded from the microphone module with a sampling frequency of 32768. The obtained raw amplitude values are in the range of 0-4096 due to the ADC bit depth (12 bits), thus, taking into account the operating range of 0…3.3 V, one ADC step is equal to 0.81 mV.

Sound image of what is happening there was not constant: it varied depending on pressure, temperature, external environment.

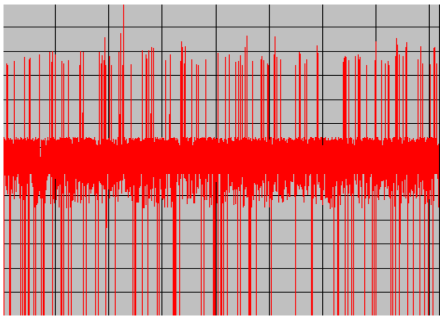

Fig. 16. Sample of phase transition water from supercritical state 08/31/2021 22:13:22 (relative unit, µs)

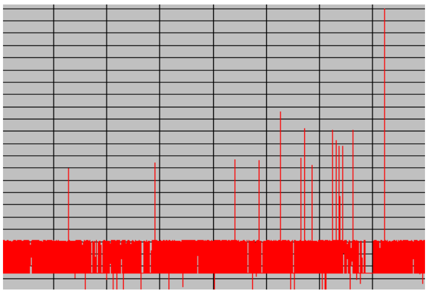

Fig. 17. Sample of phase transition water to supercritical state 08/31/2021 16:09:18 (relative units, µs)

Raw data obtained from IC in this way was not too informative (Figs. 16, 17). Also according to this data it was impossible to adequately analyze transition process or detect events of supercritical transition. Using FFT algorithm (Fast Fourier transformation) raw data for every second of measurements split into a spectrum. According to a Nyquist frequency a snapshot of the spectrum took the range from 10 Hz to 16 kHz (Figs. 18, 19). Next came the search of supercritical transition problem. To solve given problem the reference average spectrum was created. The one was computed from period when all the equipment worked normally and was not accompanied by fluid transitions from supercritical state and vice versa (Fig. 20).

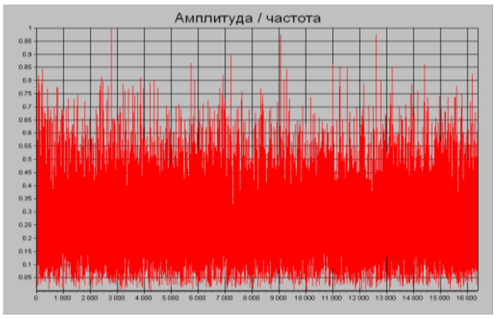

Fig. 18. Spectrum of phase transition water from supercritical state 08/31/2021 22:13:22 (relative units, Hz)

Fig. 19. Spectrum of phase transition water to supercritical state 08/31/2021 16:09:18 (relative units, Hz)

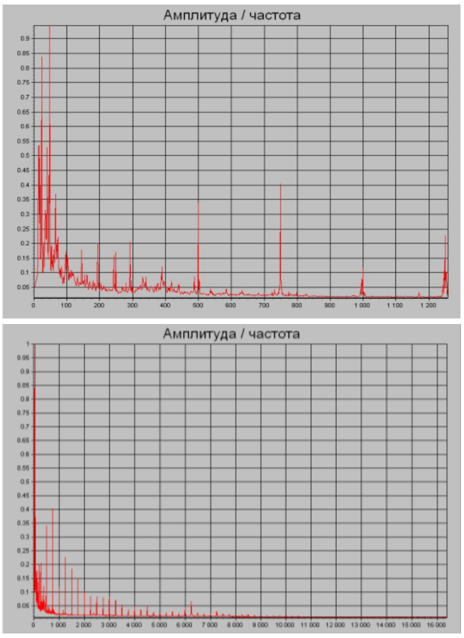

a

b

Fig. 20. Reference spectrum 0-1000 Hz (relative units, Hz) (a).
Full reference spectrum (relative units, Hz) (b)

This spectrum was used as reference in the developed program which methodically went through the files second by second and recorded Chi-square deviation from the reference spectrum corresponding specified second. So there were received charts of Chi-square deviation over experiment time. Received data simplified search long-term (longer than a few minutes) water transitions from or to the supercritical state.

In the process of examining the Chi-square graphs of the deviation (Fig. 21) in the most obvious cases of liquid phase transition, confirmed by other devices measuring pressure and temperature, a pattern was discovered.

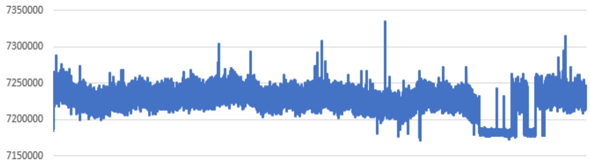

Fig. 21. Chart of Chi-square deviation for 08/31/2021 ($\chi 2$ deviation, seconds)

During the diagnostic process, it was noted that when water transitions from a supercritical state, there is a sharp increase in the amplitude of sound throughout the entire range under study in the form of white noise (see Figs. 16, 18). Also during the phase transition of the liquid to the supercritical state, the sound picture changed: the microphone picked up briefly increasing peaks in some frequency ranges (see Fig. 19). These could be either single bursts of a strictly defined frequency, or a sound simultaneously containing a "pack" of frequencies within a hundred hertz. There are usually three such peaks during transition, rarely two. At the moment of transition, their amplitude sharply increases, after which within 1…6 s it fades to average values.

Further, when analyzing the Chi-square deviation graphs, all places suspicious for such a phase transition (containing statistical outliers) are reviewed manually; if the above-described signs are present, a conclusion is drawn about the event of the transition of water to a supercritical state. In addition to long-term cases confirmed by other devices (mostly recording cases of exit from the supercritical state for more than 5 min), short-term transitions lasting 1…6 s were also detected. It was also discovered that such short transitions can occur in series several times, apparently if the installation is in boundary conditions. For the supercritical water loop used in the experiment, the following frequency bursts with a range of 100 Hz are most typical: 3.5, 4.8, 7.2, 8.4, 9.5 kHz (Fig. 22). In the process of examining Chi-square plots, 32 cases of liquid phase transition have been processed so far.

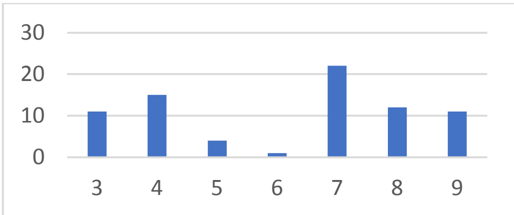

Fig. 22. Statistical sample of frequencies (repetition rate, frequencies (kHz))

CONCLUSIONS

During the study, patterns of acoustic frequencies of the transition of liquid into supercritical state were discovered for the SCWL "Loop-1c".

The software and hardware acoustic complex can be used in reactors both to monitor the operation of equipment based on the general acoustic picture (since many devices during operation emit acoustic waves that are unique to them) [21] and to diagnose the state of the coolant in closed water circuits, which are difficult to analyze by other methods from – due to the aggressiveness of the environment, temperature and ionizing radiation.

REFERENCES

1. U.S. Doe. Nuclear Energy Research Advisory Committee and Generation IV International Forum. A Technology Roadmap for Generation IV Nuclear Energy System (GIF-002-00). December 2002.
2. R.B. Duffey, H.F. Khartabil, I.L Pioro, J.M. Hopwood. The future of nuclear: SCWR Generation IV high performance channels // *Proc. of the 11th Int. Conf. on Nuclear Engineering (ICONE-11)*, Shinjuku, Tokyo, Japan, April 20-23, 2003, № 36222, 8 p.
3. I.L. Pioro, R.B. Duffey. *Heat transfer and hydraulic resistance at supercritical pressures in power-engineering applications*. New York: "ASME PRESS", 2007, p. 334.
4. K.P. Boyle, D. Brady, D. Guzonas, H. Khartabil, et al. Canada's Generation IV national program – overview // *Proc. of 4th Int. Symposium on Supercritical Water-Cooled Reactors*, March 8-11, 2009, Heidelberg, Germany, Paper № 74, 13.
5. Supercritical Water-cooled Reactor, report of SCWR System Steering Committee // *12th INPRO Dialogue Forum* (Vienna, Austria, Apri1 13-15, 2016), p. 66.
6. https://www.nextbigfuture.com/2014/06/china-seriously-looking-at.html.
7. I.G. Sharaevsky, N.M. Fialko, L.B. Zimin, et al. World trends of construction development of water-cooled supercritical pressure reactors // *Nuclear Power and the Environment*. 2020, № 2(17), p. 3-14. doi.org/10.31717/2311-8253.20.2.1.
8. V.M. Makhin, A.N. Churkin. Conceptual Proposals on Supercritical Water-cooled Reactor (overview of foreign and Russian SCWR designs) // *Problems of Atomic Science and Engineering. Series "Physics of Nuclear Reactors"*. 2017, № 1, p. 48-65.
9. Weishu Wang, Lingwei Guo, Ge Zhu, et al. *Experimental Investigation on Heat Transfer of Supercritical Water Flowing in the Subchannel with Grid Spacer in Supercritical Water-Cooled Reactor*. February 2020, Energies 13(5):1016. DOI: 10.3390/en13051016.
10. M.H. Anderson, J.R. Licht, M.L. Corradini. Progress on the University of Wisconsin super-critical water heat transfer facility // *Proc. of the 11th Int. Topical on Nuclear Reactor Thermal-Hydraulics (NURETH 11)*. Avignon, France, October 2-6, 2005, p. 265.
11. P. Hajek, R. Vsolak, M. Ruzickova. First experience with operating the supercritical water loop // *Proc. of 4th Int. Symposium on Supercritical Water-Cooled Reactors*. March 8-11, 2009, Heidelberg, Germany, Paper № 69, 10 p.
12. A.S. Bakai, V.N. Boriskin, A.N. Dovbnya, S.V. Dyuldya, D. Guzonas. Supercritical Water Convection Loop (NSC KIPT) for materials assessment for the next generation reactors // *Proc. of the 5th Int. Symposium on Supercritical Water-Cooled Reactors (ISSCWR-5)*. Vancouver, British Columbia, Canada. On CD-ROM. March 13-16, 2011, № 51, 14 p.
13. D.E. Bray, D. McBride. Nondestructive testing techniques // *Acoustic Emission Technology*. New York: John Wiley and Sons. 1992, Chapter 12, p. 345-347.
14. A.S. Bakai. Combined effect of molten fluoride salt and irradiation on Ni-based alloys // *Proc. of the NATO Advanced Study Institute on Materials Issues for Generation IV Systems: Status, Open Questions and Challenges*. Cargese, Corsica, France, Sept. 24-Oct. 6, 2007, Springer Netherlands. 2008, v. XV, p. 537-557.
15. O.S. Bakai, V.M. Boriskin, A.M. Dovbnya, et al. Combined Effect of Irradiation. Temperature, and Water Coolant Flow on Corrosion of Zr-, Ni-Cr, and Fe-Cr-based Alloys, Trans. of the ASME, J. // *Nucl. Eng. Rad. Sci*. 2016, v. 2(1), p. 021007. doi:10.1115/1.4031126.
16. .A.S. Bakai, V.N. Boriskin, A.N. Dovbnya, et al. Supercritical Water Convection Loop for SCWR materials corrosion tests under electron irradiation: First results and lessons learned // *Proc. of the 6th Int. Symp. on SCWR's (ISSCWR-6)*. 2013, Shenzhen, Guangdong, China. Paper #ISSCWR6-13062, 14 p.
17. O.S. Bakai, V.M. Boriskin, M.I. Bratchenko, S.V. Dyuldya. Electron Irradiation, temperature, and stress effect on corrosion of Zr-, Ni-Cr-, and Fe-Cr-based alloys near the water coolant supercritical transition // *Problems of Atomic Science and Technology. Series "Vacuum, Pure Materials and Superconductors"*. 2020, № 1, p. 68-77.
18. O.S. Bakai, V.N. Boriskin, M.I. Bratchenko, S.V. Dyuldya. Computational Dosimetry and Post-Irradiation Studies of the Electron Beam Irradiation Assisted Corrosion and Stress Corrosion Cracking of Statically Strained Steel Samples in a Supercritical Water Coolant // *Problems of Atomic Science and Technology. Series "Vacuum, Pure Materials and Superconductors"*. 2022, № 1, p. 55-63.
19. O.S. Bakai, V.M. Boriskin, R.M. Dronov, et al. A device for studying the durability of structural materials in the volume with the working environment // *Application for an invention of Ukraine*. № a202003423 dated 06/05/2020. The patent was published on 12.07.2023, Bull. № 28/2023.
20. V.N. Boriskin, V.V. Zakutin, N.G. Reshetniak, et al. Visualization of Electron Beam Image // *Problems of Atomic Science and Technology. Series "Nuclear Physics Investigations"*. 2014, № 3, p. 208-210.
21. V.N. Boriskin, V.V. Churikov, V.O. Momot. Development of a device and software complex for acoustic diagnostics of processes occurring in the supercritical state of a liquid and monitoring the work of a magnetic drive unit // *Problems of Atomic Science and Technology. Series "Nuclear Physics Investigations"*. 2022, № 5, p. 141-145.

Article received 11.10.2023

АКУСТИЧНА ДІАГНОСТИКА ФАЗОВИХ ПЕРЕХОДІВ ТЕПЛОНОСІЯ В НАДКРИТИЧНІЙ КОНВЕКЦІЙНІЙ ВОДЯНІЙ ПЕТЛІ

О.С. Бакай, В.М. Борискін, В.В. Чуриков

При виборі теплоносія для реакторів 4-го покоління вивчається вода в надкритичному стані. Одним із методів дослідження обрано акустичний метод, який є оптимальним за даних умов. Описано вимоги до пристрою, виконання пристрою, процес розробки програмного комплексу та результати роботи.